INTERNATIONAL JOURNAL OF HYDROGEN ENERGY XXX (2018) 1–9

Available online at www.sciencedirect.com

ScienceDirect

journal homepage: www.elsevier.com/locate/he

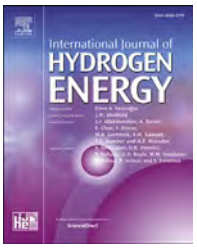

Effect of hydrogen additive on methane decomposition to hydrogen and carbon over activated carbon catalyst

Jiaofei Wang, Lijun Jin, Yang Li, Mingyi Wang, Haoquan Hu *

State Key Laboratory of Fine Chemicals, Institute of Coal Chemical Engineering, School of Chemical Engineering, Dalian University of Technology, Dalian 116024, Liaoning, China

ARTICLE INFO

Article history:
Received 3 December 2017
Received in revised form
23 July 2018
Accepted 27 July 2018
Available online xxx

Keywords:
Methane decomposition
Activated carbon
Hydrogen
Filamentous carbon

ABSTRACT

The effect of H_2 addition on CH_4 decomposition over activated carbon (AC) catalyst was investigated. The results show that the addition of H_2 to CH_4 changes both methane conversion over AC and the properties of carbon deposits produced from methane decomposition. The initial methane conversion declines from 6.6% to 3.3% with the increasing H_2 flowrate from 0 to 25 mL/min, while the methane conversion in steady stage increases first and then decreases with the flowrate of H_2, and when the H_2 flowrate is 10 mL/min, i.e. quarter flowrate of methane, the methane conversion over AC in steady stage is four times more than that without hydrogen addition. It seems that the activity and stability of catalyst are improved by the introduction of H_2 to CH_4 and the catalyst deactivation is restrained. Filamentous carbon is obtained when H_2 is introduced into CH_4 reaction gas compared with the agglomerate carbon without H_2 addition. The formation of filamentous carbon on the surface of AC and slower decrease rate of surface area and pores volume may cause the stable activity of AC during methane decomposition.

Introduction

Hydrogen is a clean fuel and considered as an attractive alternative for fossil fuels and renewable energy sources. Generally, the main sources of hydrogen are fossil fuels, water, and methane, in which fossil fuels are also the main source of air pollution that causes considerable damage to the environment. Conventionally, most of the industrial hydrogen production is based on the steam methane reforming (SMR) process, however, large amount of carbon oxides as by-product leads to the increasing cost of hydrogen production because of the necessary purification process [1,2]. Electrochemical splitting of water is a process to produce hydrogen without CO_x emission, and some efficient catalysts have been developed to improve the efficiency of process and reduce the production cost [3–7].

Catalytic methane decomposition (CMD), another simple and promising process for production of hydrogen and carbon material without by-products CO and CO_2, has received more and more attention. Many metal catalysts, such as Fe [8–10], Co [11–13] and Ni [14–16], were introduced into the process and proved as effective catalysts to promote methane decomposition. However, metal catalysts easily suffer the deactivation because the carbon deposition produced from methane encapsulates the surface active site of metals

* *Corresponding author.*
E-mail address: hhu@dlut.edu.cn (H. Hu).

https://doi.org/10.1016/j.ijhydene.2018.07.179

[17–19]. In comparison, carbon materials are considered as the alternative catalysts for methane decomposition to hydrogen owing to several advantages compared with metal catalysts such as low cost, high-temperature resistance, tolerance to sulfur and other potentially harmful impurities in the feedstock, and so on [20,21]. Activated carbon (AC) and carbon black are considered as more catalytically active materials than the more ordered ones such as graphite, diamond, carbon fibers and the carbon nanotubes [20,22], in which AC exhibits higher initial activity but lower sustainability. The rapid deactivation of AC catalysts is due to the blocking of the mouth of AC pores by growing carbon crystallites, which are generally in irregular agglomerate form [21,23]. Regeneration of carbon catalysts by carbonaceous deposit combustion with multiple cycles of reaction/regeneration or continuous supply of CO_2/H_2O to methane decomposition can effectively remove the carbon deposits and recover the carbon catalysts [24–26]. However, the regeneration of carbon catalysts will lead to the generation of undesirable CO_x and even destroy the catalyst itself [27]. The type of carbon deposition is confirmed to be an important factor to influence the activity of catalyst during methane decomposition [19]. If the deposited carbon with higher activity is obtained and the production of the deposits with low activity is suppressed, the sustainability of AC for catalytic methane decomposition could be improved without regeneration. Muradov et al. [20] found that the activity of carbon deposition produced by decomposition of various hydrocarbons toward methane decomposition reaction are different. Many researchers added various hydrocarbons, such as ethylene [28,29], ethane [30], propane [20,31], ethanol [32], etc. to methane for improving the methane decomposition over carbon. They believed that the addition of hydrocarbons to methane will affect both the activity of carbon deposits and the methane decomposition. Malaika et al. [33] reported on hydrogen production by propylene-assisted decomposition of methane over activated carbon catalysts. They found that the addition of propylene to the CDM system effectively reduces deactivation of AC and permits fast stabilization of their catalytic activity at a high level, owing to the generation of carbonaceous deposit that can be catalytically active in CDM. However, it is inevitable to produce many other kinds of gases during the decomposition with addition of other hydrocarbons, which will complicate the separation process of products to obtain pure hydrogen and increase the cost. The addition of hydrogen in reaction system has been reported to remove the carbon deposits. Otsuka et al. [34] studied the catalytic decomposition of light alkanes, alkenes and acetylene over Ni/SiO_2, and found that the hydrogenation of the carbon deposits produced by different hydrocarbons could be performed at 773 K by introducing and circulating hydrogen and only CH_4 was formed from these carbons. Bao et al. [35] and other workers [36,37] also considered that not all the coke but a part inert one causes the catalyst deactivation and the hydrogenation of inert coke facilitates the effective removal of coke and helps to revert the catalyst activity.

The addition of hydrogen in methane also affects the type and amount of carbon deposits, and the catalytic performance of catalysts in CMD. Kuvshinov et al. [38–40] investigated the effect of CH_4–H_2 mixture composition and reaction temperature on catalytic filamentous carbon formation in methane decomposition over Ni-containing catalyst. They found that the texture of the produced catalytic filamentous carbon could be changed by varying the H_2 concentration. The amount of carbon deposition was also greatly enhanced by the H_2 addition. Therefore, H_2 plays an important role on the formation of carbon deposits and improving the activity of Ni-based catalysts during methane decomposition. However, few studies were reported about the effect of H_2 on the catalytic performance of AC for methane decomposition and the properties of resultant carbon deposits. In this paper, the effect of H_2 addition amount in methane on hydrogen production and carbon formation from CH_4–H_2 mixture over ACs were investigated.

Experimental

Catalysts

AC was used as the catalyst for catalytic CH_4–H_2 mixture decomposition (CMHD). Shenmu coal, a bituminous coal from China, was used as the carbon precursor and KOH (Shantou Xilong Chemical Technology Co., China) as the activation agent for preparation of AC. The coal was physically mixed with KOH in a mass ratio of 1:2. Thereafter, the mixture was carbonized in a horizontal furnace under nitrogen atmosphere with a flow rate of 110 mL/min. Carbonization procedures and washing methods were described elsewhere [41] with the only difference on carbonization temperature of 850 °C in this work. The resultant AC was labelled as SM-AC.

Characterization

X-ray diffraction (XRD) patterns of the samples were obtained by a D/MAX-2400 with a Cu Kα radiation at 30 kV and 30 mA. Scanning electron microscopy (SEM, QUANTA 450) was conducted to record the morphology images of AC samples before and after CMD reaction. Temperature-programmed reduction (TPR) was performed in a conventional apparatus equipped with a thermal conductivity detector. About 0.03 g sample was preheated at 400 °C for 30 min before cooling to 120 °C under Ar atmosphere, then heated to 950 °C at a heating rate of 5 °C/min under pure H_2 atmosphere. The gas product was collected and analyzed by an online gas chromatograph. Raman spectra of fresh and spent ACs were measured at room temperature by using a laser Raman spectrometer (DXR Microscope). The textural properties of the samples were measured by N_2 adsorption at 77 K with a physical adsorption apparatus (ASAP 2420). The specific surface area was obtained by Brunauer-Emmett-Teller (BET) and the micropore volume (V_{mic}) calculated by using t-plot method. Thermogravimetric (TG) analysis of the samples was conducted under the air flow of 60 mL/min in a TG analyzer (Mettler Toledo TGA/SDTA851^e) to identify types of carbon deposits generated from CMHD.

CH_4–H_2 decomposition reaction

CMHD was carried out in a vertical fixed-bed reactor at atmospheric pressure. The reactor charged with 0.2 g catalyst was first heated to 850 °C under nitrogen atmosphere, and

Please cite this article in press as: Wang J, et al., Effect of hydrogen additive on methane decomposition to hydrogen and carbon over activated carbon catalyst, International Journal of Hydrogen Energy (2018), https://doi.org/10.1016/j.ijhydene.2018.07.179

then the mixture gas with 40 mL/min methane and a certain flowrate hydrogen was introduced into reactor with pure N_2. The total volumetric hourly space velocity was set at 30,000 mL/(h·g_{cat}) and the total flowrate of three gases (N_2/CH_4/H_2) was 100 mL/min. The flowrate of hydrogen is controlled at 0–25 mL/min. The effluent composition was analyzed by an online gas chromatograph (Techcomp, GC7890II) equipped with a thermal conductivity detector (packed with 5 A molecular sieve) and a flame ionization detector (GDX502 packed column). The spent catalysts containing AC and deposited carbon are named as SM-AC-xH_2, here *x* stands for H_2 flowrate. Methane conversion, hydrogen output rate and hydrogen selectivity were calculated by the following formulas:

$$X_{CH_4} = \left(F_{CH_4,in} - F_{CH_4,out}\right)/F_{CH_4,in} \times 100\% \quad (1)$$

$$Y_{H_2,out} = \left(F_{H_2,out} - F_{H_2,in}\right)/m \quad (2)$$

$$S_{H_2,out} = \left(F_{H_2,out} - F_{H_2,in}\right)/2\left(F_{CH_4,in} - F_{CH_4,out}\right) \times 100\% \quad (3)$$

where *X*, *Y*, *S*, *F*, *m* represents the methane conversion, hydrogen output rate, hydrogen selectivity, gas flowrate, and catalyst mass, respectively.

Results and discussion

Effect of H_2 flowrate on methane decomposition

Fig. 1a and b present the time dependence of methane conversion and hydrogen output rate in CMHD over SM-AC, respectively. It is observed that methane conversion and hydrogen output rate sharply decrease in initial reaction period, then decline slowly with time in the presence or absence of H_2. In the presence of H_2, the initial methane conversion and hydrogen output rate are smaller than that without H_2 because the addition of hydrogen increases the content of target product in reaction system, which will restrain the conversion of methane to hydrogen in terms of thermodynamics and kinetics. However, the addition of H_2 to CH_4 obviously influences the stability. When no H_2 is added, the methane conversion decreases from 6.6% to 0.6% and hydrogen output rate from 1.1 mmol/(g_{cat}·min) to 0.085 mmol/(g_{cat}·min) after 360 min of reaction. Although declining in initial period, the methane conversion and hydrogen output rate keeps at least 1.8% and 0.27 mmol/(g_{cat}·min), respectively, after 400 min of CMHD reaction. As the H_2 flowrate increases from 0 to 10 mL/min, the final methane conversion increases from 0.6% to 2.7% after 375 min of reaction. However, when the H_2 flowrate is further enhanced to 25 mL/min, the initial methane conversion declines to 3.3% and maintains at 1.8% after 410 min of reaction. It is concluded that the introduction of part hydrogen is helpful to methane decomposition and catalytic stability, but the excessive hydrogen will be unfavorable to the decomposition owing to the reverse reaction of CMD. As seen from Fig. 1b, similar trend is obtained for the dependence of hydrogen output rate on flowrate of hydrogen addition and reaction time.

The addition of hydrogen to methane not only improves the methane conversion and hydrogen output rate, but also increases the hydrogen selectivity during methane decomposition. As shown in Fig. 1c, the hydrogen selectivity declines from 97% to 84% with the lapse of time when no hydrogen is added. The remarkable decrease of methane conversion with time on stream causes the dramatic decrease of hydrogen content, while the content of by-products, mainly C_2H_4 and

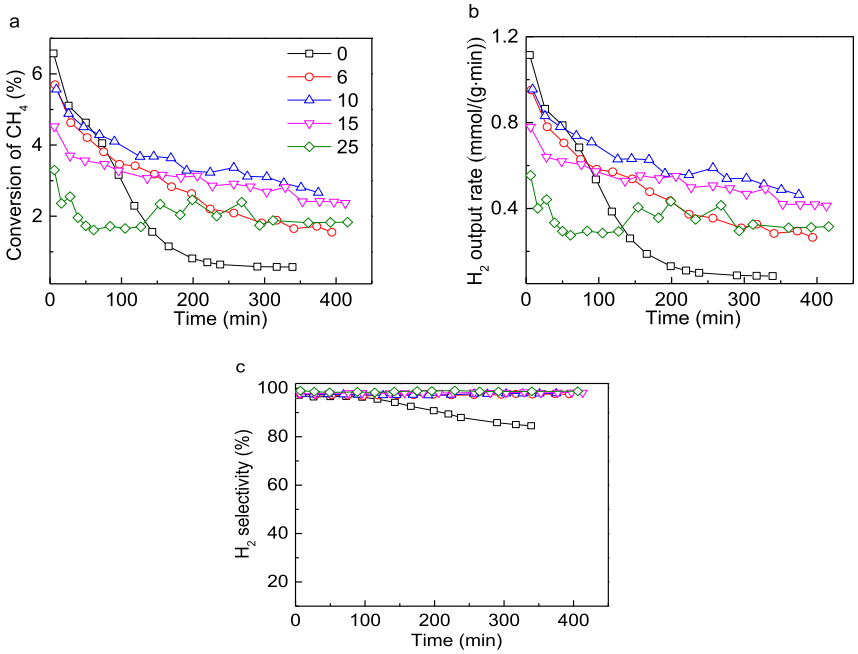

Fig. 1 – Methane conversion, hydrogen output rate and hydrogen selectivity in CMHD with different H_2 flowrate over SM-AC. (Reaction conditions: reaction temperature, 850 °C, catalyst mass, 0.2 g, total flowrate, 100 mL/min, space velocity, 30,000 mL/(h·g_{cat}), flowrate of CH_4, 40 mL/min).

Please cite this article in press as: Wang J, et al., Effect of hydrogen additive on methane decomposition to hydrogen and carbon over activated carbon catalyst, International Journal of Hydrogen Energy (2018), https://doi.org/10.1016/j.ijhydene.2018.07.179

C_2H_6, decreases less than that of hydrogen. Therefore, the hydrogen selectivity decreases as the reduction of methane conversion. However, the hydrogen selectivity changes little with time on stream, and even increases a little when hydrogen is introduced into methane. This indicates that the introduction of hydrogen promotes the conversion of methane to hydrogen rather than other by-products such as C_2H_4 and C_2H_6, which may be attributed to the ability of hydrogen to stabilize the methyl or methylene and thus suppressing the formation of C_2H_4 or C_2H_6 by the integrating of the methyl or methylene.

Fig. 2 illustrates the XRD patterns of fresh and spent SM-AC in CMHD reaction. It is observed that the intensity of peaks ascribed to carbon in the XRD patterns of the spent catalysts increases, meaning the formation of carbon deposits on surface of SM-AC during the decomposition reactions. Compared with the SM-AC-$0H_2$, the peak (26°) attributed to graphite carbon appears on the spent catalysts when H_2 is introduced into CH_4, indicating that the addition of H_2 to CH_4 changes the type of carbon deposits from methane decomposition. With the increasing flowrate of H_2, the peak intensity of carbon at 26° changes, implying that the crystal properties of carbon deposits change with the introducing amount of hydrogen, which may be a factor impacting the activity of carbon catalysts [28,29]. What's more, the trend of the peak intensity of carbon deposits changing with hydrogen flowrate is similar to that of methane conversion and hydrogen output rate, which also indicates that the activity of SM-AC may be affected by the type or the crystal structure of the carbon deposit on the surface of SM-AC produced from methane decomposition.

It is clear that the agglomerate carbon deposits are formed on the surface of SM-AC when no hydrogen is added to methane, as shown in SEM images (Fig. 3), while some filamentous carbons are generated on the surface of SM-AC-$10H_2$ and SM-AC-$25H_2$ along with the presence of some agglomerate deposits. That the filamentous carbon deposit is directly generated from methane decomposition over AC catalysts has been reported only on few researches [42–44]. When the hydrogen flowrate increases from 10 mL/min to 25 mL/min, i.e. quarter to five eighths of methane flowrate, the proportion of filamentous carbon on the surface of AC further increases. In the SEM images of SM-AC-$10H_2$ and SM-AC-$25H_2$, almost the same diameter ranges of the filamentous carbons (25–65 nm) can be found despite the different H_2 flowrate. It is concluded that the presence of hydrogen in methane favors the generation of filamentous carbon and restricts the formation of agglomerate carbon deposit from methane decomposition. The filamentous carbon grows more orderly on the surface than the agglomerate one, which may expose more active surface and give the methane more access to the active site on surface of AC catalyst. However, when the addition amount of hydrogen to methane is too large, such as 25 mL/min, the strong inhibition effect of hydrogen on methane decomposition in terms of thermodynamics and kinetics results in lower methane conversion although the catalysts have higher activity.

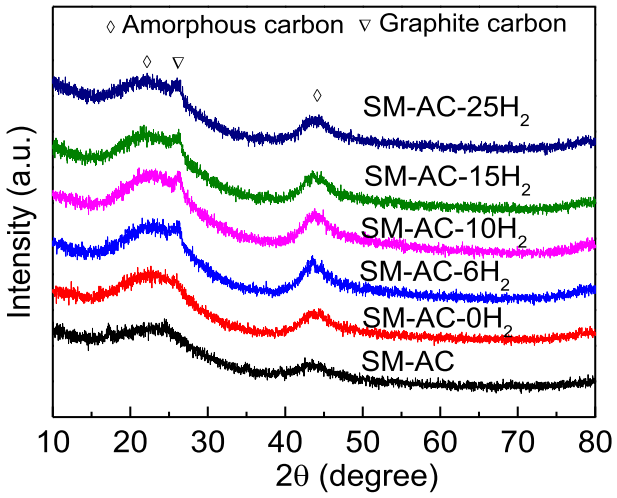

Fig. 2 – XRD patterns of fresh catalysts and spent SM-AC catalysts in CMHD with different H_2 flowrate. (SM-AC-xH_2: the spent catalysts containing SM-AC and deposited carbon, here x is flowrate of H_2 added to methane).

TG and DTG curves of SM-AC and SM-AC-xH_2 under air atmosphere are shown in Fig. 4. The temperature corresponding to the maximum weight loss rate (T_{max}) of SM-AC is about 530 °C, while the T_{max} of SM-AC-xH_2 increases to about 670 °C, obviously higher than the former, indicating that the SM-AC-xH_2 or the carbon deposits formed during methane decomposition has lower oxidation reactivity than SM-AC. In addition, when the hydrogen is added to methane, the T_{max} of SM-AC-xH_2 decreases with the increase of hydrogen flowrate, which is related to the different textural properties of SM-AC-xH_2 and types of carbon deposits generated from CMHD.

Raman spectra was utilized to clarify the structure of the deposited carbons over AC. For all the carbon samples, two main bands are observed at 1340 ± 10 cm^{-1} (D band) and 1590 ± 10 cm^{-1} (G band), as shown in Fig. 5. The G band is attributed to the in-plane carbon-carbon stretching vibrations of graphite layers, while the D band is ascribed to the structural imperfection of graphite [45,46]. To better identify the different structure of carbons deposition, curve fitting technique was taken [47,48]. Four Gaussian peaks can be seen in first order Raman process of fitting Raman spectra (see in Fig. 6), where the G mode in ACs gives rise to a multi-peak feature named G1 and G2; and D mode to two peaks named D1 and D2. The fitting parameters obtained from fitting two Gaussians as G and D bands to the Raman spectra are listed in Table 1. The position of G1 and D1 are close to those of G (~1580 cm^{-1}) and D (~1345 cm^{-1}), being ascribed to in-plane stretching and breathing vibration modes from the basal planes, while G2 and D2 with lower frequency are ascribed to sp^2 clusters like a-Cs with bond angle disorder [34].

The peak intensity ratio of I(G2)/I(G1) is considered as a parameter to express the relative content of the bond angle disorder to order in AC materials [48,49], and the higher the I(G2)/I(G1), the higher degree of disorder. The lower I(G2)/I(G1) ratio of the spent AC catalysts than that of fresh AC, imply that the more ordered carbon deposits are produced from methane decomposition, and spent SM-ACs have more ordered structure compared with fresh one. The difference of I(G2)/I(G1) ratio among the spent ACs under different H_2 flowrate means the different disorder degree of structure. This indicates that different types of carbon deposits can be obtained through

Please cite this article in press as: Wang J, et al., Effect of hydrogen additive on methane decomposition to hydrogen and carbon over activated carbon catalyst, International Journal of Hydrogen Energy (2018), https://doi.org/10.1016/j.ijhydene.2018.07.179

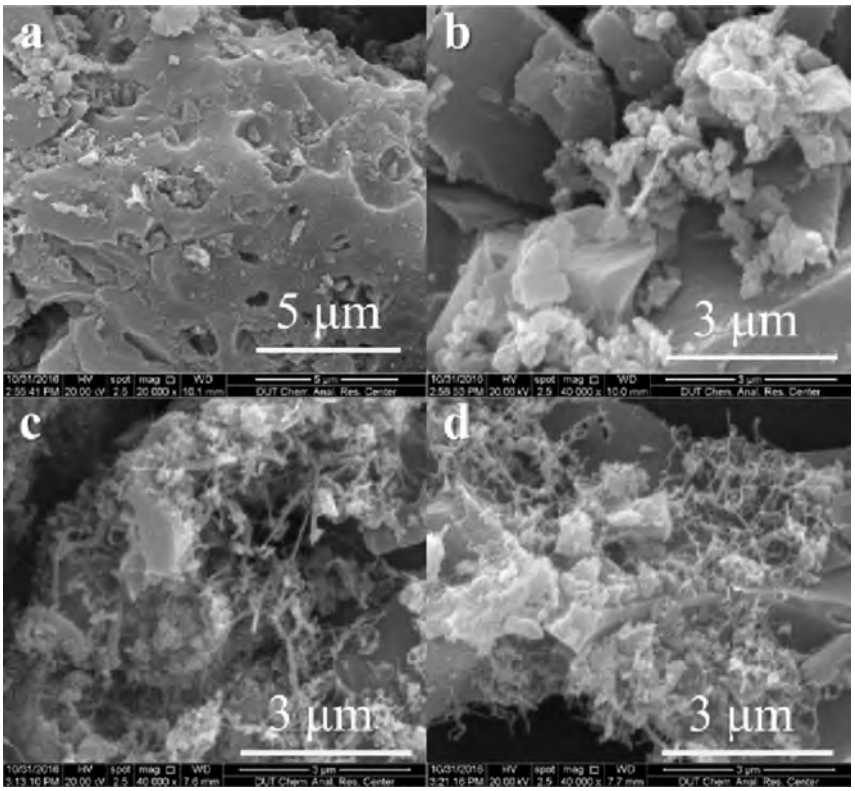

Fig. 3 – SEM images of fresh and spent SM-AC. (a) Fresh SM-AC, (b) SM-AC-0H_2, (c) SM-AC-10H_2, (d) SM-AC-25H_2.

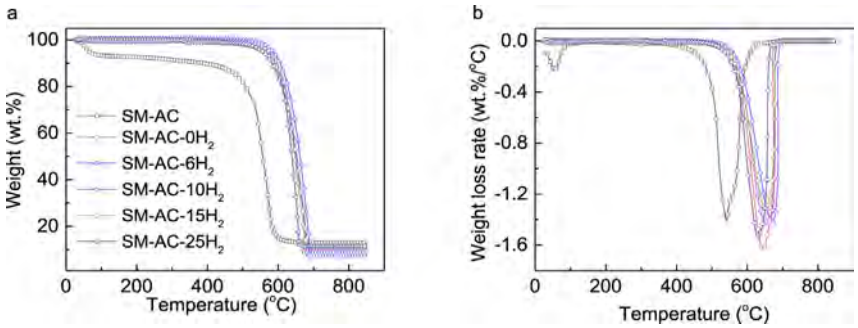

Fig. 4 – TG and DTG curves of fresh and spent SM-AC in air (TG condition: flowrate of air, 60 mL/min; heating rate, 10 °C/min).

adding hydrogen to methane and changing the H_2 flowrate, which is consistent with the results of SEM. The I(G2)/I(G1) ratio increases firstly with the H_2 flowrate and then decreases when H_2 flowrate is up to 25 mL/min, which seems similar to the changes of methane conversion with H_2 flowrate, except for 15 mL/min. This implies that there may present a relationship between the I(G2)/I(G1) ratio and the activity of the catalyst. Lower methane conversion over SM-AC in 15 mL/min of H_2 flowrate than that in 10 mL/min of H_2 flowrate may be due to greater suppression to methane decomposition caused by higher H_2 flowrate although the SM-AC-15H_2 has higher I(G2)/I(G1) ratio than SM-AC-10H_2. Similar regularity can also be obtained from the analysis of the width of D1 band, which correlates well with the degree of disorder over the entire order-disorder interval [50]. Muradov et al. [20,22] believed that disordered carbons are, in general, more catalytically active than the ordered ones. Therefore, owing to the formation of filamentous carbon deposits over AC, better stability was obtained when H_2 is added to CH_4 for catalytic decomposition of methane.

Table 2 lists the textural properties of fresh and spent SM-AC. The specific surface area of SM-AC significantly decreases after the methane decomposition with or without hydrogen addition because the pores are blocked by the carbon produced from methane decomposition, which is also an important factor causing the deactivation of SM-AC [44,51]. As for SM-AC-0H_2 and SM-AC-6H_2, the surface area is less than 10 m^2/g, attributed to the blocking of the pores of SM-AC by carbon deposits, and thus the activity of the carbon catalysts and methane conversion are very low in steady state. However, when the flowrate of hydrogen is up to 10 mL/min and 15 mL/min, the specific surface area of spent SM-AC increases

Please cite this article in press as: Wang J, et al., Effect of hydrogen additive on methane decomposition to hydrogen and carbon over activated carbon catalyst, International Journal of Hydrogen Energy (2018), https://doi.org/10.1016/j.ijhydene.2018.07.179

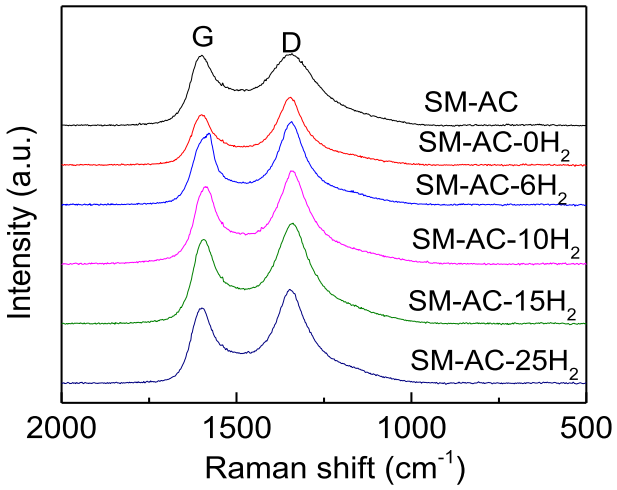

Fig. 5 – Raman spectra of fresh and spent SM-AC in CMHD with different H_2 flowrate.

obviously. This indicates that the surface area, pore or active sites of AC may lose slower when a certain amount of hydrogen is added, and the activity of carbon catalyst is partly kept, leading to higher methane conversion and hydrogen out rate. Especially, the specific surface area of SM-AC-25H_2 is 721 m^2/g, significantly higher than that of other spent SM-ACs and part of pores are not blocked. However, the methane conversion of SM-AC-25H_2 is much less than that of other spent SM-ACs in CMHD reaction, indicating that the methane decomposition is suppressed by large amount of hydrogen even though the surface area, pore, and active sites of SM-ACs are remained. What's more, although SM-AC-0H_2 and SM-AC-6H_2 have similar specific surface area, the methane conversion over SM-AC-6H_2 is higher than that over SM-AC-0H_2, indicating that the addition of hydrogen to methane may promote the methane decomposition. It is thought that higher methane conversion may be from two aspects when hydrogen is added to methane. One is that the specific surface area, pore or the active sites of AC lose slower when hydrogen is added

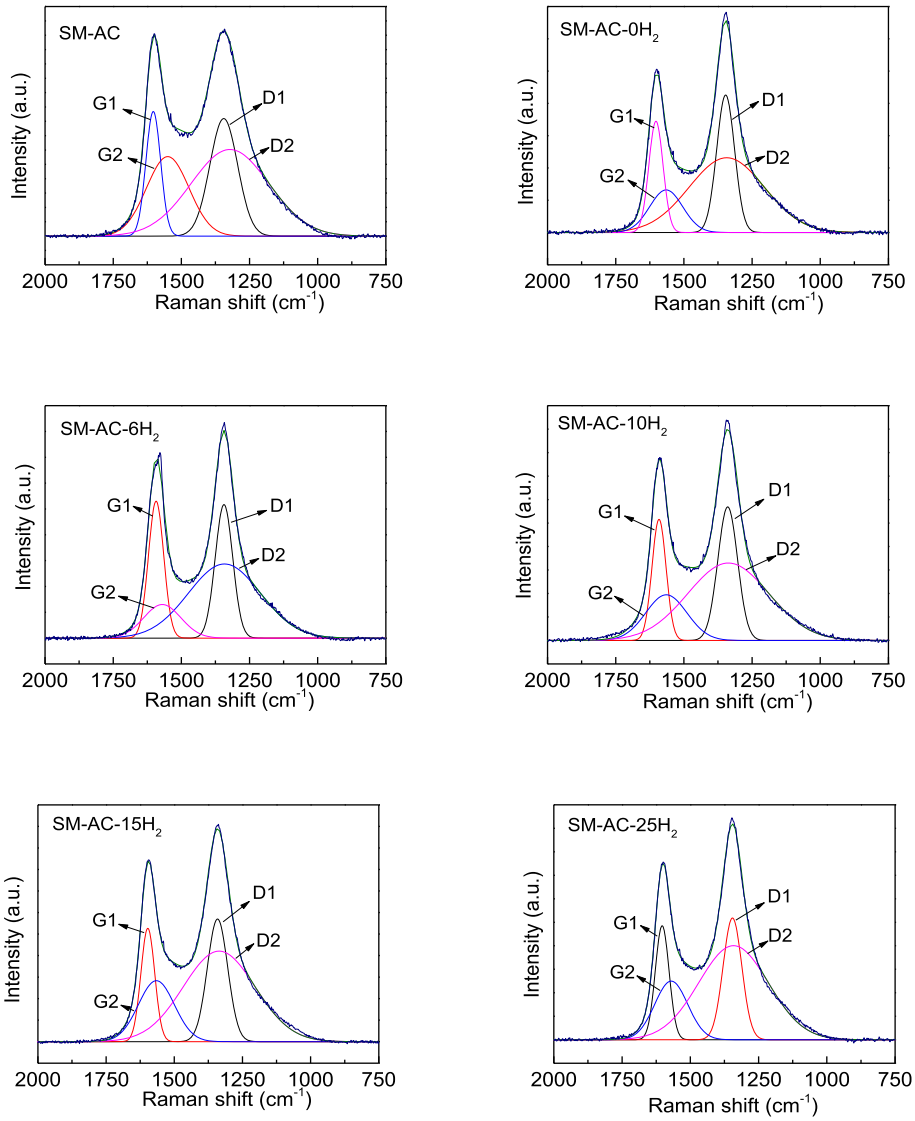

Fig. 6 – Raman spectra with fitting results by using four Gaussians for fresh and spent SM-AC in CMHD with different H_2 flowrate.

Please cite this article in press as: Wang J, et al., Effect of hydrogen additive on methane decomposition to hydrogen and carbon over activated carbon catalyst, International Journal of Hydrogen Energy (2018), https://doi.org/10.1016/j.ijhydene.2018.07.179

Table 1 – Fitting parameters of spent catalysts obtained from fitting four Gaussians (G1, G2, D1, and D2) of the Raman spectra.

Samples[a]	G1		G2		D1		D2		I(G2)/I(G1)
	$\upsilon(cm^{-1})$	$\Gamma(cm^{-1})$	$\upsilon(cm^{-1})$	$\Gamma(cm^{-1})$	$\upsilon(cm^{-1})$	$\Gamma(cm^{-1})$	$\upsilon(cm^{-1})$	$\Gamma(cm^{-1})$	
SM-AC	1603	63	1550	184	1345	120	1322	336	1.85
SM-AC-0H_2	1602	62	1565	143	1347	77	1343	325	0.89
SM-AC-6H_2	1592	67	1557	201	1344	77	1327	300	0.72
SM-AC-10H_2	1591	61	1564	178	1339	85	1337	350	1.22
SM-AC-15H_2	1597	60	1566	156	1341	88	1335	310	1.34
SM-AC-25H_2	1603	59	1570	142	1346	81	1342	300	1.18

υ the center position of peak.
Γ the full width at half maximum.
[a] SM-AC-xH_2 stands for the spent catalysts containing SM-AC and deposited carbon, here x is flowrate of H_2 added to methane.

Table 2 – Textural properties of fresh and spent SM-AC.

Sample	S_{BET} (m^2/g)	S_{mic} (m^2/g)	S_{ext} (m^2/g)	V_t (cm^3/g)	V_{mic} (cm^3/g)
SM-AC	1535	1055	480	0.76	0.49
SM-AC-0H_2	8.6	–	8.6	0.08	–
SM-AC-6H_2	9.7	–	9.7	0.08	–
SM-AC-10H_2	57.6	2.0	55.6	0.10	0.003
SM-AC-15H_2	42.2	–	42.2	0.11	–
SM-AC-25H_2	721	618	103	0.40	0.26

because of the inhibition effect of hydrogen on methane decomposition; and another is the different activity of the SM-AC with different types of carbon deposits. It is well known that the structure and surface defects serve as active sites in methane decomposition over carbon catalysts [20]. According to the results of Raman spectra shown in Table 1, the SM-AC covered by filamentous carbon from CMHD is more disorder than that by agglomerate carbon deposits, and the former has higher activity. Therefore, higher methane conversion and stability were obtained in H_2–CH_4 gases.

To sum up, when hydrogen is added to the methane, the effect on methane decomposition are in two aspects, the inhibition effect on methane decomposition because of thermodynamics and kinetics, and the improvement of catalytic stability of activated carbon catalyst. The former will lower methane conversion and the latter will increase methane conversion. If the former effect is weaker than the latter, the methane conversion will be enhanced, otherwise, the methane conversion will decrease. When the addition amount of hydrogen is more than 15 mL/min, the inhibition effect is greater than the improvement of catalytic stability of carbon catalysts; therefore, the methane conversion is lower than that with 10 mL/min of hydrogen addition to methane.

Formation of filamentous carbon

Usually, filamentous carbon is formed on metal catalysts in methane decomposition [8,11,15,52], which is caused by the driving force of the pronounced gradient of carbon concentration existing between the front and trailing faces of the metal particles. However, few works reported on the formation of filamentous carbon on carbon catalysts, especially on AC. Zhang et al. [44] reported that fibrous carbons were produced in methane decomposition over hierarchical micro-/macro-mesoporous carbons from CLR. They believed that the special pore structure and the limited oxygen content of the carbon are responsible for the formation and growth of fibrous carbons. Suelves et al. [42] used different carbon blacks as catalysts for methane decomposition and found that carbon filaments appeared on the surface of HS-50 after reaction. They considered that the presence of metallic impurities is the cause for formation of carbon filaments. However, these two causes mentioned above may be not the main reasons for the formation of filamentous carbon in this work because the catalysts used in CMD and CMHD are identical, and the formation of filamentous carbon happens only when H_2 is added.

Fig. 7 shows the TPR curves of fresh SM-AC and spent SM-AC. It is clearly observed that a peak at 400–700 °C appears for SM-AC, but the peak disappears for the spent SM-ACs, which suggests almost consumption of oxygen-containing surface groups during the methane decomposition [41,53,54]. There seems no other difference presenting between the TPR curves of spent catalyst in CMD and that in CMHD, except for a weak peak from 450 to 500 °C for SM-AC-10H_2 and SM-AC-25H_2. It is inferred that a little oxygen containing surface group of SM-AC is still remained after CMHD reaction, which may promote the activation of methane and sustain the activity of SM-AC.

It can be assumed that the hydrogen introduced to methane limits the formation of agglomerate carbon deposits,

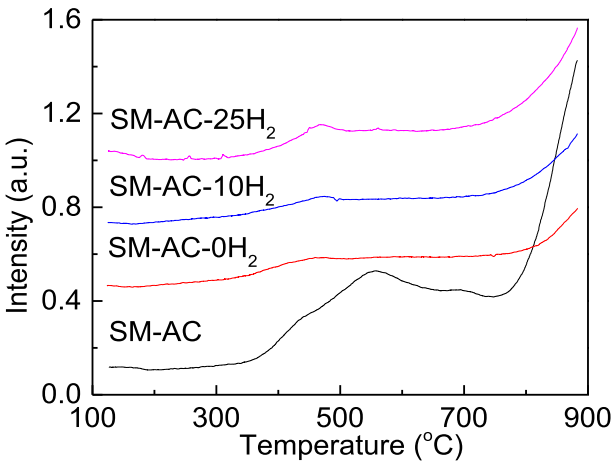

Fig. 7 – TPR curves of fresh and spent SM-AC catalysts in CMHD with different H_2 flowrate.

Please cite this article in press as: Wang J, et al., Effect of hydrogen additive on methane decomposition to hydrogen and carbon over activated carbon catalyst, International Journal of Hydrogen Energy (2018), https://doi.org/10.1016/j.ijhydene.2018.07.179

but promotes the growth of filamentous carbon. That is to say, the presence of hydrogen is the main reason for the formation of filamentous carbon. The competitive adsorption of hydrogen and methane causes the methane to occupy less active sites on surface of AC, and the active sites adsorbing methane molecule may be separated and isolated by those adsorbing hydrogen molecule. The formation rate of carbon crystal nucleus are decreased by the presence of hydrogen, and the crystal nucleus is less possibly aggregated with each other. According to thermodynamics equilibrium, the introduction of hydrogen partly restrains the decomposition of methane, slows down the decomposition, and the rate of carbon nucleus formation decreases, which also may prevent the sharply deactivation of AC and the formation of agglomerate deposits. While the sustained activity of AC promotes the decomposition of methane, the formation and growth of crystal nucleus. The mechanism and further reason of the formation of filamentous carbon are not clear. We considered that the conflict between inhibition of hydrogen addition and promotion of activity carbon to methane decomposition may cause the formation of filamentous carbon.

Conclusions

The addition of hydrogen in methane obviously influences the catalytic performances of SM-AC and the carbon structure formed from methane decomposition. The stability of the carbon catalyst was significantly improved although the initial activity of SM-AC decreased when a certain amount of hydrogen was added to methane. The addition of hydrogen improves the methane decomposition over SM-AC but restricts the reaction at excessive amount. What's more, the filamentous carbon deposits are formed on surface of the AC catalyst with the introduction of hydrogen into methane besides the production of irregularly agglomerate carbon deposits. The part of surface area and pores are remained after CMHD, which may be the cause for higher stability of SM-AC in the presence of hydrogen. The combined action of the competitive adsorption of hydrogen and methane, the promotion of AC catalyst, and the inhibition of hydrogen to methane decomposition leads to the generation of filamentous carbon and limits the formation of irregularly agglomerate carbon deposits.

Acknowledgements

This work was supported by Joint Fund of NSFC and Xinjiang Provincial Government (No. U1503194), the NSFC (No. 21576046), the Joint Fund of Coal-based Low Hydrocarbons by NSFC and Shanxi Provincial Government (No. U1510101), and Natural Science Fund of Liaoning (No. 20170540180).

REFERENCES

[1] Bayat N, Rezaei M, Meshkani F. Methane decomposition over Ni-Fe/Al_2O_3 catalysts for production of CO_x-free hydrogen and carbon nanofiber. Int J Hydrogen Energy 2016;41:1574–84.
[2] Chesnokov VV, Chichkan AS. Production of hydrogen by methane catalytic decomposition over Ni-Cu-Fe/Al_2O_3 catalyst. Int J Hydrogen Energy 2009;34:2979–85.
[3] Wang J, Zhong HX, Wang ZL, Meng FL, Zhang XB. Integrated three-dimensional carbon paper/carbon tubes/cobalt-sulfide sheets as an efficient electrode for overall water splitting. ACS Nano 2016;10:2342–8.
[4] Wang J, Li K, Zhong HX, Xu D, Wang ZL, Jiang Z, et al. Synergistic effect between metal-nitrogen-carbon sheets and NiO nanoparticles for enhanced electrochemical water-oxidation performance. Angew Chem 2015;54:10530–4.
[5] Liu K, Zhong H, Li S, Duan Y, Shi M, Zhang X, et al. Advanced catalysts for sustainable hydrogen generation and storage via hydrogen evolution and carbon dioxide/nitrogen reduction reactions. Prog Mater Sci 2018;92:64–111.
[6] Wang ZL, Hao XF, Jiang Z, Sun XP, Xu D, Wang J, et al. C and N hybrid coordination derived Co-C-N complex as a highly efficient electrocatalyst for hydrogen evolution reaction. J Am Chem Soc 2015;137:15070–3.
[7] Meng F, Zhong H, Bao D, Yan J, Zhang X. In situ coupling of strung Co_4N and intertwined N-C fibers toward free-standing bifunctional cathode for robust, efficient, and flexible Zn-air batteries. J Am Chem Soc 2016;138:10226–31.
[8] Takenaka S. Formation of filamentous carbons over supported Fe catalysts through methane decomposition. J Catal 2004;222:520–31.
[9] Sivakumar V, Mohamed A, Abdullah A, Chai SP. Influence of a Fe/activated carbon catalyst and reaction parameters on methane decomposition during the synthesis of carbon nanotubes. Chem Pap 2010;64:799–805.
[10] Jin L, Si H, Zhang J, Lin P, Hu Z, Qiu B, et al. Preparation of activated carbon supported Fe-Al_2O_3 catalyst and its application for hydrogen production by catalytic methane decomposition. Int J Hydrogen Energy 2013;38:10373–80.
[11] Nuernberg GB, Fajardo HV, Mezalira DZ, Casarin TJ, Probst LFD, Carreño NLV. Preparation and evaluation of Co/Al_2O_3 catalysts in the production of hydrogen from thermocatalytic decomposition of methane: influence of operating conditions on catalyst performance. Fuel 2008;87:1698–704.
[12] Italiano G, Delia A, Espro C, Bonura G, Frusteri F. Methane decomposition over Co thin layer supported catalysts to produce hydrogen for fuel cell. Int J Hydrogen Energy 2010;35:11568–75.
[13] Jana P, de la Peña O'Shea VA, Coronado JM, Serrano DP. Cobalt based catalysts prepared by Pechini method for CO_2-free hydrogen production by methane decomposition. Int J Hydrogen Energy 2010;35:10285–94.
[14] Takenaka S, Ogihara H, Otsuka K. Structural change of Ni species in Ni/SiO_2 catalyst during decomposition of methane. J Catal 2002;208:54–63.
[15] Chen D, Christensen K, Ochoafernandez E, Yu Z, Totdal B, Latorre N, et al. Synthesis of carbon nanofibers: effects of Ni crystal size during methane decomposition. J Catal 2005;229:82–96.
[16] Pudukudy M, Yaakob Z. Methane decomposition over Ni, Co and Fe based monometallic catalysts supported on sol gel derived SiO_2 microflakes. Chem Eng J 2015;262:1009–21.
[17] Li Y, Li D, Wang G. Methane decomposition to CO_x-free hydrogen and nano-carbon material on group 8-10 base metal catalysts: a review. Catal Today 2011;162:1–48.
[18] Rostrup-Nielsen JR. Mechanisms of carbon formation on nickel-containing catalysts. J Catal 1977;48:155–65.
[19] Demicheli MC, Ponzi EN, Ferretti OA, Yeramian AA. Kinetics of carbon formation from CH_4-H_2 mixtures on nickel-alumina catalyst. Chem Eng J 1991;46:129–36.
[20] Muradov N, Smith F, T-Raissi A. Catalytic activity of carbons for methane decomposition reaction. Catal Today 2005;102–103:225–33.

Please cite this article in press as: Wang J, et al., Effect of hydrogen additive on methane decomposition to hydrogen and carbon over activated carbon catalyst, International Journal of Hydrogen Energy (2018), https://doi.org/10.1016/j.ijhydene.2018.07.179

[21] Bai Z, Chen H, Li B, Li W. Catalytic decomposition of methane over activated carbon. J Anal Appl Pyrol 2005;73:335–41.
[22] Muradov N. Catalysis of methane decomposition over elemental carbon. Catal Commun 2001;2:89–94.
[23] Ashok J, Kumar SN, Venugopal A, Kumari VD, Tripathi S, Subrahmanyam M. CO_x free hydrogen by methane decomposition over activated carbons. Catal Commun 2008;9:164–9.
[24] Abbas HF, Daud WMAW. Thermocatalytic decomposition of methane for hydrogen production using activated carbon catalyst: regeneration and characterization studies. Int J Hydrogen Energy 2009;34:8034–45.
[25] Abbas HF, Daud WMAW. An experimental investigation into the CO_2 gasification of deactivated activated-carbon catalyst used for methane decomposition to produce hydrogen. Int J Hydrogen Energy 2010;35:141–50.
[26] Muradov N, Chen Z, Smith F. Fossil hydrogen with reduced emission: modeling thermocatalytic decomposition of methane in a fluidized bed of carbon particles. Int J Hydrogen Energy 2005;30:1149–58.
[27] Adamska A, Malaika A, Kozzowski M. Carbon-catalyzed decomposition of methane in the presence of carbon dioxide. Energy Fuels 2010;24:3307–12.
[28] Takehira K, Ohi T, Shishido T, Kawabata T, Takaki K. Catalytic growth of carbon fibers from methane and ethylene on carbon-supported Ni catalysts. Appl Catal A Gen 2005;283:137–45.
[29] Malaika A, Kozłowski M. Influence of ethylene on carbon-catalysed decomposition of methane. Int J Hydrogen Energy 2009;34:2600–5.
[30] Kim MS, Lee SY, Kwak JH, Han GY, Yoon KJ. Hydrogen production by decomposition of ethane-containing methane over carbon black catalysts. Kor J Chem Eng 2011;28:1833–8.
[31] Pinilla JL, Suelves I, Lázaro MJ, Moliner R. Influence on hydrogen production of the minor components of natural gas during its decomposition using carbonaceous catalysts. J Power Sources 2009;192:100–6.
[32] Rechnia P, Malaika A, Najder-Kozdrowska L, Kozłowski M. The effect of ethanol on carbon-catalysed decomposition of methane. Int J Hydrogen Energy 2012;37:7512–20.
[33] Malaika A, Kozlowski M. Hydrogen production by propylene-assisted decomposition of methane over activated carbon catalysts. Int J Hydrogen Energy 2010;35:10302–10.
[34] Otsuka K, Kobayashi S, Takenaka S. Hydrogen-deuterium exchange studies on the decomposition of methane over Ni/SiO_2. J Catal 2001;200:4–9.
[35] Sun C, Fang G, Guo X, Hu Y, Ma S, Yang T, et al. Methane dehydroaromatization with periodic CH_4-H_2 switch: a promising process for aromatics and hydrogen. J Energy Chem 2015;24:257–63.
[36] Honda K, Yoshida T, Zhang ZG. Methane dehydroaromatization over Mo/HZSM-5 in periodic CH_4-H_2 switching operation mode. Catal Commun 2003;4:21–6.
[37] Honda K, Chen X, Zhang ZG. Preparation of highly active binder-added MoO_3/HZSM-5 catalyst for the non-oxidative dehydroaromatization of methane. Appl Catal A Gen 2008;351:122–30.
[38] Kuvshinov GG, Mogilnykh YI, Kuvshinov DG, Zaikovskii VI, Avdeeva LB. Peculiarities of filamentous carbon formation in mehtane decomposition on Ni-containing catalysts. Carbon 1998;36:87–97.
[39] Kuvshinov GG, Mogilnykh YI, Kuvshinov DG. Kinetics of carbon formation from CH_4-H_2 mixtures over a nickel containing catalyst. Catal Today 1998;42:357–60.
[40] Zavarukhin SG, Kuvshinov GG. The kinetic model of formation of nanofibrous carbon from CH_4-H_2 mixture over a high-loaded nickel catalyst with consideration for the catalyst deactivation. Appl Catal A Gen 2004;272:219–27.
[41] Wang J, Jin L, Li Y, Jia C, Hu H. Effect of air pre-oxidization on coal-based activated carbon for methane decomposition to hydrogen. Int J Hydrogen Energy 2016;41:10661–9.
[42] Suelves I, Lázaro MJ, Moliner R, Pinilla JL, Cubero H. Hydrogen production by methane decarbonization: carbonaceous catalysts. Int J Hydrogen Energy 2007;32:3320–6.
[43] Fidalgo B, Fernández Y, Zubizarreta L, Arenillas A, Domínguez A, Pis JJ, et al. Growth of nanofilaments on carbon-based materials from microwave-assisted decomposition of CH_4. Appl Surf Sci 2008;254:3553–7.
[44] Zhang J, Jin L, Li Y, Si H, Qiu B, Hu H. Hierarchical porous carbon catalyst for simultaneous preparation of hydrogen and fibrous carbon by catalytic methane decomposition. Int J Hydrogen Energy 2013;38:8732–40.
[45] Otsuka K, Kobayashi S, Takenaka S. Catalytic decomposition of light alkanes, alkenes and acetylene over Ni/SiO_2. Appl Catal A Gen 2001;210:371–9.
[46] Dresselhaus MS, Jorio A, Hofmann M, Dresselhaus G, Saito R. Perspectives on carbon nanotubes and graphene Raman spectroscopy. Nano Lett 2010;10:751–8.
[47] Beeman D, Silverman J, Lynds R, Anderson MR. Modeling studies of amorphous carbon. Phys Rev B 1984;30:870–5.
[48] Shimodaira N, Masui A. Raman spectroscopic investigations of activated carbon materials. J Appl Phys 2002;92:902.
[49] Ferrari AC, Robertson J. Interpretation of Raman spectra of disordered and amorphous carbon. Phys Rev B 2000;61:14095–106.
[50] Cuesta A, Dhamelincourt P, Laureyns J, Martinez-Alonso A, Tascon JMD. Raman microprobe studies on carbon materials. Carbon 1994;32:1523–32.
[51] Serrano DP, Botas JÁ, Pizarro P, Gómez G. Kinetic and autocatalytic effects during the hydrogen production by methane decomposition over carbonaceous catalysts. Int J Hydrogen Energy 2013;38:5671–83.
[52] Zhang J, Jin L, Li Y, Hu H. Ni doped carbons for hydrogen production by catalytic methane decomposition. Int J Hydrogen Energy 2013;38:3937–47.
[53] Moliner RSI, Lazaro MJ, Moreno O. Thermocatalytic decomposition of methane over activatedin'uence of textural properties and surface chemistry. Int J Hydrogen Energy 2005;30:293–300.
[54] Fidalgo B, MenÉNdez JÁ. Carbon materials as catalysts for decomposition and CO_2 reforming of methane: a review. Chin J Catal 2011;32:207–16.

Please cite this article in press as: Wang J, et al., Effect of hydrogen additive on methane decomposition to hydrogen and carbon over activated carbon catalyst, International Journal of Hydrogen Energy (2018), https://doi.org/10.1016/j.ijhydene.2018.07.179